Study of Biomass Combustion Wastes

Roberto García, Consuelo Pizarro*, Ana Álvarez, Antonio G. Lavín, Julio L. Bueno

Department of Chemical and Environmental Engineering. Faculty of Chemistry.

University of Oviedo. Julián Clavería s/n. 33006. Oviedo. Spain

*corresponding author

telephone: +34 985103438

fax: +34 985103434

e-mail: pizarroconsuelo@uniovi.es

Abstract

A number of widely referenced environmental and logistic advantages suggest biomass as an interesting feedstock to obtain energy in large quantities. One of the most important problems when using biomass is the amount of solid wastes produced, which causes deposition and corrosion phenomena (slagging and fouling) entailing energy efficiency decrement and maintenance problems.

This work focuses on the study of ashes from eighteen different biomass samples, including energy crops, agricultural, industrial and forestry wastes and commercial fuels.

Morphology (SEM) and grain size (PSD-LD) studies showed a homogeneous structure with low quantities of health risky fine particles for most samples after 550ºC burning. Compositional studies (EDXA, XRF) suggested that some of the studied samples, such as almond shell or rice husk, may respectively present high deposition and corrosion risks.

Keywords

Biomass ash, ternary diagrams, XRF, SEM, particle size distribution, TGA

1. Introduction

Constant growth in mankind's energy requirements over the last century in addition to the high dependence on fossil fuels has outlined important environmental challenges. In this scenario, renewable energy sources appear to be a sustainable tool to complement and gradually substitute fossil fuels in energy production. Among them, biomass, regarded as a feedstock for thermal conversion, presents some advantages such as its neutrality concerning CO_2 emissions during its life cycle [1] or its low N and S content that entails low NO_x and SO_2 emissions [2]. Besides this, biomass is considered as an autonomous resource which partially avoids foreign energy dependence [3]. Because of the advantages when using biomass for energy production, it has experienced a huge development in recent years.Nevertheless, it also presents some disadvantages, being one of the most important the generation of solid wastes [4]. Ash presence is highly negative for the combustion process as it involves energy efficiency losses and higher maintenance expenses due to *unburnts* and depositions (*slagging* and *fouling*) that cause thermal resistances in heat exchangers, corrosion phenomena and the increase of fumes and aerosol emissions [5, 6].

Ashes generated during the biomass combustion may present a variable composition with a wide range of mineral and inorganic components included in its structure. These can proceed from the vegetal biomass itself or from other contaminants added during pre-treatment or transport phases. Because of this, any quality control criterion suggests the exhaustive knowledge of ash characteristics, both morphological and compositional.

To that aim, there are several analytical techniques available, commonly used by several authors that supply complete information about biomass samples. In that way **Scanning Electron Microscopy** (**SEM**) coupled to an **Energy Dispersive X-Ray Analyzer** (**EDXA**) allows simultaneous morphological and semi-quantitative compositional information of the studied sample. Biagini [7] and Umamaheswaran [8] use these techniques to study the structural variations of some biomass fuel after combustion processes. Xiao [9] evaluates the structural evolution of biomass ashes after different ashing temperatures. Nortey Yeboah [10] characterizes coal ashes with high carbon content that will be later co-fired with biomass. Carrasco [11] uses SEM to characterize bottom ash from biomass to use in concrete formulation and Abraham [12] studies several ash samples trying to find reuse for them in fertilizer, cement or pollutant adsorbent industries. Wang S. [13] employs EDXA to obtain the elemental composition of biomass fly ash.

Sample's morphology and grain size information can be obtained by developing **Particle size distribution** (**PSD**). Bridgeman [14] and Mediavilla [15] sieved and weighted fractions of biomass fuels to study the effect of raw materials size on combustion properties and kinetic parameters, respectively. Becidan [16] determined fly ash grain distribution, by previously dividing them in size cuts using an Electrical Low Pressure Impactor. Roy [17] studied particle size distributions of biomass samples by direct measure on SEM images and Wang G. [18] did the same to fly ashes by laser diffraction (LD).

To obtain chemical composition data other techniques besides EDXA can be used. One of the most common is **X-Ray Fluorescence** (**XRF**). Reviews fromVassilev [19, 20] provide plenty of information about the elementary composition of several biomass samples. Some other authors also use this technique to study the biomass-ash deposition

tendency of different ashes by using predictive coefficients [21, 22] or ternary diagrams [23, 24].

Thermo Gravimetrical Analysis (**TGA)** is used by several authors to thermally analyze different biomass samples and determine characteristic points in their burning profiles such as their ignition point, peak temperature, burn out temperature [25, 26] or kinetic parameters [27]. Our research group has recently proposed a mechanism to obtain proximate analysis data by using this analytical tool [28].

This work focuses on obtaining ash behaviour data of several different biomass samples and comparing them in order to determine which ones would be most suitable for use in further combustion processes.

2. Materials and methods

2.1 Samples

In this work, eighteen different biomass samples were tested after air dried and grinded to assure homogeneity. They were chosen as represent all the classification groups, e.g. as these suggested by Ávila [29]. Energy crops (sorghum –S- and thistle –THI-), agricultural feedstocks (beetroot pellets –BP-, straw pellets –SP- and rice husk –RH-,), industrial sources (almond shell –AS-, coffee husk –CH-, olive stone –OS-, pine kernel shell –PKS- and vine orujillo –VO-) and forestry wastes (olive tree pruning –OTP-, pine apple leaf –PL-, and vine shoot chips –VSC-). In addition to this some of the most common commercial fuels currently available at the Spanish market were studied (briquette –BRI-, charcoal –CC-, pine and pine apple leaf pellets –PPLP-, wood chips –WC- and wood pellets –WP-)

General combustion-data for these samples is provided in Table 1. Their ashes obtained at 550ºC were also studied. This temperature was chosen as it is considered by several

100 authors [30, 31, 32] to be the optimum one to determine their properties. Proximate and
101 ultimate analysis data and higher heating values (HHV) are summarized from previous
102 works by this research group [33].

103 **2.2 Experimental equipment**

104 **SEM** images were obtained, in this work, using a MEB JEOL-6100 equipment coupled
105 to an INCA Energy 200 EDX analyser, to simultaneously obtain 3D images and semi-
106 quantitative elemental analyses. To this aim samples were previously air dried and
107 grinded under 500 µm and covered with a thin gold layer, as they must be conductant.
108 **Particle size distribution** was developed with a laser diffractometer Malvern
109 Intrument'sMastersizer S2000. Samples were originally burned at 550ºC and the residue
110 grinded to avoid coalescence, and measure real particle size
111 **XRF** data was obtained using Phillips PW2404 equipment joined to a PW2540
112 automatic sample loader. Samples ashes were obtained at 550ºC and later burnt at
113 900ºC in order to obtain the mineral matter. Nine elements data (Si, Al, Fe, Mn, Mg,
114 Ca, Na, K, Ti and P) were obtained, considered as oxides in its highest oxidation level.
115 TGA experiments were developed in a Perkin Elmer STA 6000 thermobalance, using
116 10mg of sample and a slow heating rate (5ºC/min) from room temperature up to 900ºC
117 in an oxidant air-atmosphere with an air flow of 40 ml/min.

118 **3. Theory and calculation**

119 Slagging and fouling are two phenomena, directly related to deposition and corrosion,
120 commonly observed when operating a biomass-powered combustion system. The first
121 of them is produced at high temperature zones, mainly on grills or chamber walls,
122 whilst the second istypical of low temperature zones, like the heat exchanger surfaces.
123 They depend on the fuel's chemical composition, conversion technology used and
124 operating conditions [19].

XRF data is a useful tool to calculate some deposition-predictive indexes, some of which are included in Table 2, as this phenomenon is usually increased by high concentrations of low melting point elements, like Na, K, S, Cl (alkali sulphates or chlorides) and decreased by high melting point ones such as Ca, Mg or S (calcium or magnesium silicates).

4. Results and discussion

4.1 Morphology and size

Due to space requirements, only the **SEM images** that show the most relevant facts are included in this work. In this way a yellow marked fibrous structure can be observed in the wood chips sample (figure 1). This is due to the high lignin levels of woody fuels which make them harder and more difficult to grind homogenously. Structural holes (blue) that confer this fuel a high specific surface but low density, are also detected. On the other hand, harder samples such as pine kernel shell (Figure 2a) present, before burning, isolated particles of high size and quite regular sphere-shape. Those two effects co-exist in the pine and pine apple leaf pellets sample (Figure 2b and 2c) which is a mix between a woody fuel and a harder one. Images observed after 550ºC treatment changes due to thermal effect are easily seen. At this point structural chemical bonding has been broken so hemicellulose, cellulose and lignin of most biomass samples have turned into gaseous CO_2 and CH_4 having lost up to 70% of their initial weight, giving a finely divided structure. Some particles are outlined (orange) in this structure are unburnts, formed by alkali sulphates with high melting points not vaporized at low temperatures that gain relative weight at high temperatures.Low melting point elements may also agglomerate forming particle clusters and high melting temperature compounds.

Concerning **particle size distribution,** ash particles can be classified in *thin* or *thick* if they, respectively, cross or do not cross a 400 µm mesh sieve [11]. Fly ash is usually

considered to have a diameter between 0.2 and 200 μm and bottom ash as between 200 and 1000 μm [35]. The concept PM10 (particulate matter 10) meansthe quantity of particles under10 μm that float in the atmosphere polluting its composition. This group includes the PM2.5 (particulate matter 2.5 μm) ones, or *breathable particles*, that can affect human health by penetrating human airways. In this work, PSD results obtained by laser diffraction, are divided in five ranges (under 10, 10-100, 100-200, 200-400 and over 400 μm) and their results compared. It is interesting for ashes to have as higher thick or bottom ash fractions as possible (more than 200 μm particles) that are easily removed from the bottom of the chambers, avoiding contamination and health damage risks. As can be seen in Figure 3 most of the studied samples have more than 80 % of ash particles thicker than 200 μm, beetroot pellets, pine and pine-apple pine pellets or vine orujillo more than 90 % of them. On the other hand wood pellets and almond shell were found to have, respectively, 35 and 45 % of particles under fly ash considered diameter. None of the samples presented PM10 values over 3% and PM2.5 detected values were negligible in every case, with only charcoal and pine kernel shell samples reaching 0.1 %.

4.2 Chemical composition

Figure 4 presents the results obtained for **EDXA analysis** after 550 ºC *ashing temperature* as an average of six measure points throughout SEM-observed sample. As can be seen in Table 1, raw fuel structure is, as expected, basically organicwith a vast majority of C and O in the sample composition and a C/O ratio between 0.8 and 1 in most caseswhich is influential in biomass reactivity and indicates higher heating value.Beetroot pellets, sorghum and vine shoot chips present a ratio slightly lower,close to 0.7 and rice husk far under this value with a 0.38 ratio, being a highly oxygenated structure that confers low HHV to this fuel. On the other hand charcoal presents a

175 4.68C/O ratio, as it underwent a previous pyrolysis. When these data are compared
176 with the ones obtained after 550ºC burning (Figure 4), it can be highlighted that at this
177 temperature most of the carbon structure was eliminated and the proportion of high
178 melting-temperature elements has increased. C values are commonly between 15-25%
179 while O (which still remains in oxides) carbonates or sulphates has slightly increased
180 until 40-60%. Charcoal differs from these results due to the previously explained
181 reasons. Concerning other elements it is remarkable the high silicon peaks observed in
182 charcoal (40%), pine kernel shell or straw pellets (10%). K and Ca, key elements in
183 fouling and slagging generation, are also interesting being the first ones close to 5% in
184 most samples, with the exception of straw pellets (10%), charcoal (15%), pine and pine
185 apple leaf pellets (20%) or vine orujillo (30%). Ca values are slightly above K ones,
186 with olive stone, wood or beetroot pellets (10%) and charcoal (30%) above the average.
187 Mg presents a nearly constant value of 3-5% for most samples and the low Na values
188 (around 1 are the other remarkable notes. Cl values detected in the rice husk sample are
189 extremely high, reaching 30%, this may proceed from fertilizers or a bad homogeneity
190 of measure points, but there are some herbaceous species with high natural values in
191 themselves.
192 **X-Ray fluorescence** measured values are presented in Table 3. These are used to
193 calculate deposition predictive equations and their results compared with ternary
194 diagrams and experimental experience. Every predictive equation proposed in Table 3
195 was calculated and meaningful differences were noticed for the same sample. Due to
196 this, only the most referenced equations are proposed and compared in this work, one
197 to predict slag ($R_{b/a}$) and one to predict fouling (F_u), but both can be used to predict
198 general deposition and their results compared. These results are presented in Table 3
199 following a colour criterion, red, orange and green being high, medium and low

deposition risk respectively. As can be seen deposition predictions obtained from both equations agree in the samples with high and low values but present some contradictions in the intermediate ones, conceding high or medium deposition risk in some cases depending on the considered equation. When these results are compared with the ones obtained by using ternary diagrams this tendency can be confirmed.

In this way when a sample presents more than 50% (mass percentage in ashes) of CaO or SiO_2 combined with more than 15% of K_2O, its ashes can easily agglomerate and therefore deposit. This means the samples on the right of the red line drawn on the SiO_2-CaO-K_2O diagram (Figure 5). As can be determined,samples AS, CC, PPLP, PL, PKS, VO and WP present high deposition risks, all of them were considered as high or medium risk by using predictive equations. Some contradictions are also noticed, for example fuels with the highest deposition predictive values like VSC, THI or CH are not supposed to present high risk according to this diagram.

The SiO_2+Al_2O_3+Fe_2O_3-+Na_2O+TiO_2-CaO+MgO+MnO-K_2O+P_2O_5+S (Figure 6) diagram is also presented. This classifies samples according to their acidity (high, medium or low) which is influential oncorrosion phenomena and melting point (S, C, K and CK types). S and K types present high deposition risks due to silicates formation and potassium presence. C type is expected to have high melting temperature (and therefore, low depositions) due to high Ca levels. CK type is an intermediate between C and K. According to this, results are quite homogeneous if compared with SiO_2-CaO-K_2O diagram ones, as they both consider PPLP, PL, PKS, SP and VO as high deposition risk samples and AS and WP as medium risk ones. The same contradictions with predictive equations as in the previous case are noticed.

When compared with experimental experience, it should be stated that most of the samples except PKS, VO and WP presented no deposition problems when burning on a

crucible. These samples are predicted as high deposition risk with both graphic methods, so they must be considered, for our tested samples, as more reliable. Regarding acidity, following the explained criterion only RH presents high acidity values, meaning high corrosion risk in the burning equipment, which agrees with high chlorine values measured by EDXA.

4.3 Thermogravimetric study

As previously stated, thermogravimetry is a versatile tool that can be used in several ways to study biomass and its wastes. One of the most common uses for the burning profile of a sample, that relates weight loss and temperature, is to determine characteristic points: ignition point, when a fuel begins to react, and peak point, when mass loss speed is the highest in the sample, related with its reactivity. Table 4 shows the characteristic points obtained for the selected samples. In this work, TGA is also use to compare different biomass samples char and ash thermal behaviour; this means when fuel's weight attains a steady speed after peak temperature, and before the reaction end, from 400 to 850 ºC.

As can be seen ignition temperature is in the range 170-200 ºC for every sample except THI,that falls 130ºC,entailing higher auto-ignition risk if appropriate conditions, like high powdery atmospheres, are reached, and WC and CC that increase until 212 and 233 ºC, respectively.

Peak temperature values, when a sudden volatile matter and a huge mass loss occur, are usually between 230-330 ºC. CC, because of its pyrolytic origin, presents a lower volatile matter quantity, and a more constant mass loss, this value increasing up to 487ºC.

Figures 7 and 8 show the mass loss of the studied sample's from 400 to 850 ºC. As can be seen, every sample (except VO and CC) has lost more than 60% of its original

weight at this relatively low temperature. In the focused range, mass loss decreases quite homogeneously until a turning point when combustion reaction ends. This one changes quite a lot depending on the selected fuel, from nearly 500ºC of PL, THI or RH to 800 ºC for AS, CC or VO. It is interesting to have a high reaction-end temperature which permits to obtain fuel yields in a wider operation range.

5. Conclusions

In this work different biomass samples have been characterized by SEM, XRD, PSD, FRX and TG in order to establish which ones are the most desirable for combustion applications.

SEM images showed that the natural structure of harder biomass fuels (shells or husks) makes them easier to homogenise andhandle, than fibrous ones (wood or straw). The ashes obtained after 550 ºC burning present a homogeneous finely-divided structure with presence of unburnt.

PSD study demonstrated that BP and PPLP generate a vast majority of thick ashes, while the selected brand of WP and AS have more than 35% of fine particles, increasing environmental and health risks with their use.

Deposition predictive equations, combined with FRX based ternary diagrams and experimental experience suggest that AS, PPLP, PL, PKS or VO present high deposition risks, decreasing the energy yield of the reaction. RH sample has huge corrosion risks due to its acidity which is confirmed by Cl presence measured by EDXA.

TG study showed that THI presented a low ignition point which has direct influence on auto-ignition and explosive atmospheres generation. AS, CC and VO present wider reaction ranges thank to their higher reaction-end temperature.

Acknowledgements

PSE-ARFRISOL, Ref. PS-120000-2005-1, is a scientific-technologic project qualified as Strategic by the 2004-07 Spanish National Plan of Research, Development and Diffusion, co-financed by the European Regional Development Funds and the Spanish Science and Education Ministry. We must acknowledge all members of the PSE-ARFRISOL partnership for their cooperation.

We also wish to thank many companies such as Pellets Asturias, Factor Verde, Molygrasa, Dibiosur, Enfosur, Acciona, Nutral Arrocerías Dorado, CarsanBio, Parque Verde, Viñadecanes Vinos, la Cooperativa Agrícola de Cangas del Narcea, Vino de la Tierra de Cangas, Gebio, Aragonesa Bioenergía and Cafés El Gallego for their disinterested collaboration supplying most of the necessary samples of the different biomasses.

This article is also greately indebted to MINECO for the economical facilities given to the project TRIBIONOR (CTQ2013-45155-R) that allows a continuity in this research field.

References

[1] Gil MV, Casal D, Pevida C, Pis JJ, Rubiera F. Thermal behaviour and kinetics of coal/biomass blends during co-combustion. Bioresource Technol 2010; 101: 5601–8.

[2] Qian FP, Chyang CS, Huang KS, Tso J. Combustion and NO emission of high nitrogen content biomass in a pilot-scale vortexing fluidized bed combustor. Bioresource Technol 2011; 102: 1892–8.

[3] Demirbas A. Importance of biomass energy sources for Turkey. Energ Policy 2008; 36: 834–2.

[4] Sebastián F, García D, Rezeau A. Energías renovables-Energía de la biomasa (volumen I). Prensas Universitarias de Zaragoza. Zaragoza. 2010.

[5] Van Loo S, Koppejan J. The handbook of biomass combustion and co-firing. Earthscan. London. 2010.

[6] Fang X, Jia L. Experimental study on ash fusion characteristics of biomass. Bioresource Technol 2012; 104: 769-4.

[7] Biagini E, Narducci P, Tognotti L. Size and structural characterization of lignin-cellulosic fuels after the rapid devolatilization. Fuel 2008; 87: 177-6.

[8] Umamaheswaran K, Batra VS. Physico-chemical characterisation of Indian biomass ashes. Fuel 2008; 87: 628–8.

[9] Xiao R, Chen X, Wang F, Yu G. The physicochemical properties of different biomass ashes at different ashing temperature. Renew energ 2011; 36: 244-9.

[10] Nortey Yeboah NN, Shearer CR, Burns SE, Kurtis KE. Characterization of biomass and high carbon content coal ash for productive reuse applications. Fuel 2014; 116: 438–7

[11] Carrasco B, Cruz N, Terrados J, Corpas FA, Pérez L. An evaluation of bottom ash from plant biomass as a replacement for cement in building blocks. Fuel 2014; 118: 272–0

[12] Abraham R, George J, Thomas J, Yusuff KKM. Physicochemical characterization and possible applications of the waste biomass ash from oleoresin industries of India. Fuel 2013; 109: 366–2.

[13] Wang S, Miller A, Llamazos E, Fonseca F, Baxter L. Biomass fly ash in concrete: Mixture proportioning and mechanical properties. Fuel 2008; 87: 365-1.

[14] Bridgeman TG, Darvell LI, Jones JM, Williams PT, Fahmi R, Bridgewater AV et al. Influence of particle size on the analytical and chemical properties of two energy crops. Fuel 2007; 86: 60-72.

[15] Mediavilla I, Fernández MJ, Esteban LS.Optimization of pelletisation and combustion in a boiler of 17.5 kW for vine shoots and industrial cork residue. Fuel Process Technol 2009; 90: 621-8.

[16] Becidan M, Todorovic D, Skreiberg O, Khalil RA, Backman R, Goile F et al. Ash related behaviour in staged and non-staged combustion of biomass fuels and fuel mixtures. Biomass Bioenerg 2012; 41: 86-3.

[17] Roy MM, Dutta A, Corscadden K. An experimental study of combustion and emissions of biomass pellets in a prototype pellet furnace. App Energ 2013; 108: 298–7.

[18] Wang G, Silva RB, Azevedo JLT, Martins-Dias S, Costa M. Evaluation of the combustion behaviour and ash characteristics of biomass waste derived fuels, pine and coal in a drop tube furnace. Fuel 2014; 117: 809–24.

[19] Vassilev SV, Baxter D, Andersen LK, Vassileva CG. An overview of the chemical composition of biomass. Fuel 2010; 89: 913–33.

[20] Vassilev SV, Baxter D, Andersen LK, Vassileva CG. An overview of the composition and application of biomass ash. Part 1.Phase–mineral and chemical composition and classification. Fuel 2013; 105: 40–76.

[21] Fryda L, Sobrino C, Glazer M, Bertrand C, Cieplik M. Study of ash deposition during coal combustion under oxyfuel conditions. Fuel 2012; 92: 308–7.

[22] Vamvuka D, Pitharoulis M, Alevizos G, Repouskou E, Pentari D. Ash effects during combustion of lignite/biomass blends in fluidized bed. Renew Energ 2009; 34: 2662–1.

[23] Fernández MJ, Carrasco JE. Comparing methods for predicting the sintering of biomass ash in combustion. Fuel 2005; 84: 1893–0.

[24] Vassilev SV, Baxter D, Andersen LK, Vassileva CG, Morgan TJ. An overview of the organic and inorganic phase composition of biomass.Fuel2012; 94: 1–33.

[25] Magdziarz A, Wilk M. Thermogravimetric study of biomass, sewage sludge and coal combustion. Energ Convers Manage 2013; 75:425–0.

[26] Sarkar P, Sahu SG, Mukherjee A, Kumar M, Adak AK, Chakraborty N et al. Co-combustion studies for potential application of sawdust or its low temperature char as co-fuel with coal. App Therm Eng 2014; 63: 616-3.

[27] VersanKok M, Özgür E. Thermal analysis and kinetics of biomass samples. Fuel Process Technol 2013; 106: 739–3

361 [28] García R, Pizarro C, Lavín AG, Bueno JL. Biomass proximate analysis
362 using thermogravimetry. Bioresource Technol 2013; 139: 1–4.

363 [29] Ávila C, Pang CH, Wu T, Lester E. Morphology and reactivity of char
364 biomass particles. Bioresource Technol 2011; 102: 5237-3.

365 [30] Fernández MJ, Carrasco JE. Concentration of elements in woody and
366 herbaceous biomass as a function of the dry ashing temperature. Fuel 2006;
367 85: 1273–9.

368 [31] Thyrel M, Samuelsson R, Finell M, Lestander TA. Critical ash elements
369 in biorefinery feedstock determined by X-ray spectroscopy. App Energ 2013;
370 102: 1288–4.

371 [32] García-Maraver A, Terron LC, Ramos-Ridao A, Zamorano M. Effects of
372 mineral contamination on the ash content of olive tree residual biomass.
373 Biosystems Eng 2014; 118: 167-3.

374 [33] García R, Pizarro C, Lavín AG, Bueno JL. Characterization of Spanish
375 biomass wastes for energy use. Bioresource Technol 2012; 103: 249–8.

376 [34] Tortosa-Masiá AA, Buhre BJP, Gupta RP, Wall TF. Characterising ash
377 of biomass and waste. Fuel ProcessTechnol2007; 88: 1071-1.

378 [35] Grammelis P, Skodras G, Kakaras E. Effects of biomass co-firing with
379 coal on ash properties. Part I: Characterisation and PSD. Fuel 2006; 85: 2310-
380 5.

Table 1

Tested fuels analytical values.

Sample	Proximate analysis				HHV	Ultimate analysis					
	M	Ash	VM	FC		N	C	S	H	O	C/O
AS	8.68	2.2	82	15.8	18275	0.3	46.35	0.22	5.67	47.46	0.98
BP	12.5	9	76	15	15095	1.19	38.94	0.51	5.23	54.13	0.72
BRI	5.84	0.8	85	14.2	18498	1.24	46.74	0.1	6.39	45.53	1.03
CC	5.29	5.9	26	68.1	29712	0.65	79.34	0.3	2.74	16.97	4.68
CH	9.6	5.8	76.2	18	18236	2.53	45.06	0.48	6.42	45.51	0.99
OS	11	1.4	78.3	20.3	17884	1.781	46.55	0.11	6.33	45.229	1.03
OTP	8.7	13	78	9	17342	1.47	45.36	0.28	5.47	47.42	0.96
PPLP	8.2	3.2	75	21.8	18147	0.4	42.26	0.27	4.81	52.26	0.81
PKS	9.14	1.3	80	18.7	18633	0.27	47.65	0.11	6.33	45.2	1.05
PL	8.33	2.7	77.6	19.7	18893	0.31	47.91	0.6	4.9	46.28	1.04
RH	7.27	13.7	74	12.3	15899	0.21	26.69	0.17	2.88	70.05	0.38
S	6.1	17	62	21	11872	0.73	37.89	0.21	5.94	55.23	0.69
SP	7.3	9.8	79	11.2	16584	0.56	47.89	0.17	5.51	45.87	1.04
TH	11.6	0.2	80.67	19.13	17747	0.48	43.89	0.28	6.46	48.89	0.90
VO	9.5	12.7	79	8.3	17742	1.91	44.15	0.58	5.31	48.05	0.92
VSC	22	9.7	66	24.3	14631	0.61	40.15	0.31	5.02	53.91	0.74
WC	25.6	1.5	68.6	29.9	15162	0.13	42.2	0.27	5.51	51.89	0.81
WP	7.7	1.3	82	16.7	18218	0.6	46.79	0.32	6.13	46.16	1.01

M. ash. VM and *FC* respectively mean moisture Ash, volatile matter and fixed carbon. Measured in mass percentage. *HHV* is the higher heating value measured in J/g. *C. N. H. O* and *S* are the mass percentage of carbon, nitrogen, hydrogen, oxygen and sulphur.

Table 2

Review of deposition-predictive indexes.

Method	Formulae	Deposition criteria
Base/acid ratio [9, 14, 21, 22]	$R_{b/a} = \frac{Fe_2O_3 + CaO + MgO + K_2O + Na_2O}{SiO_2 + TiO_2 + Al_2O_3}$ P_2O_5 may be also added as a Basic oxide [34]	< 0.5 → low 0.5-1 → medium > 1 → high
Silicon/alumina ratio [9, 14, 22]	$S/A = \frac{SiO_2}{Al_2O_3}$	<0.31 or > 3 → low 0.31-3 → high
Iron/calcium ratio [14, 22]	$I/C = \frac{Fe_2O_3}{CaO}$	<0.31 or > 3 → low 0.31-3 → high
Slagging index [14, 22]	$R_S = R_{b/a} \cdot S$	< 0.6 → low 0.6-2 → medium > 2 → high
Slag viscosity index [9, 14]	$S_R = \frac{SiO_2}{SiO_2 + Fe_2O_3 + CaO + MgO} \cdot 100$	>78 → low 66.1-78 → medium <66.1 → high
Chlorine content [14]	Weight percentage of Cl. in an "as received" fuel sample	<0.2 → low 0.2-0.3 → medium 0.3-0.5 → high >0.5 → really high
Fouling index I [14]	$F_u = R_{b/a} \cdot (K_2O + Na_2O)$	< 0.6 → low 0.6-40 → high >40 →extremely high
Fouling index II [21]	$F = \frac{K_2O + Na_2O}{2 \cdot S + Cl}$	Higher as higher F
Alkali index [14]	$IA = \frac{1}{HHV} \cdot Ash \cdot (K_2O + Na_2O)$	>0.17 → probably fouling > 0.34 → sure
I parameter [23]	$I = \frac{CaO + MgO}{K_2O + Na_2O}$	>2 no sinter
Total alkali content [14, 22]	$TA = (K_2O + Na_2O)$	<0.3 → low 0.3-0.4 → medium > 0.4 → high
H fouling index [9]	$H = R_{b/a} \cdot Na_2O$ if $\frac{Fe_2O_3}{CaO+MgO} > 1$ $H = Na_2O$ if $\frac{Fe_2O_3}{CaO+MgO} < 1$ and $CaO + MgO > 2$	<3 →medium >3 → high
Fusion temp index [18]	$F = \frac{SiO_2 + K_2O + P_2O_5}{CaO + MgO}$	Higher tendency as higher F value

Each element/oxide symbol means its weight percentage of obtained from elemental analysis (S), EDXA (Cl) or XRF (oxides). *HHV* is the higher heating value measured in GJ/kg and *ash* the ash mass percentage of the measured sample.

Table 3

X-Ray fluorescence data.

	XRF data										Equations	
	SiO_2	Al_2O_3	Fe_2O_3	MnO	MgO	CaO	Na_2O	K_2O	TiO_2	P_2O_5	$R_{b/a}$	F_u
AS	31.0	4.4	1.2	0.1	6.3	25.7	1.4	25.8	0.1	3.9	1.7	46.4
BP	42.3	5.2	1.5	0.1	6.3	35.1	1.2	4.2	0.3	3.8	1.0	5.4
BRI	24.5	9.6	1.8	1.3	7.5	39.2	1.9	10.1	1.7	2.5	1.7	20.2
CC	15.9	3.1	2.2	0.4	7.3	45.0	2.7	15.4	0.2	7.8	3.8	68.1
CH	5.3	1.5	1.9	0.4	14.4	59.4	1.5	11.5	0.1	3.9	12.8	166.8
OS	26.6	6.2	3.1	0.1	11.7	37.0	0.9	11.0	0.4	3.0	1.9	23.0
OTP	50.1	3.9	1.6	0.1	2.6	33.5	0.5	5.5	0.4	1.9	0.8	4.8
PPLP	49.2	5.6	1.1	0.1	4.9	6.5	1.3	27.1	0.1	4.1	0.7	21.2
PL	18.1	4.7	6.3	0.3	14.2	11.5	1.9	35.3	0.1	7.7	3.0	112.3
PKS	51.3	4.1	2.9	0.1	4.8	7.5	1.4	24.6	0.1	3.3	0.7	19.2
RH	88.2	1.3	0.4	0.3	1.1	1.8	0.4	4.9	0.0	1.7	0.1	0.5
S	53.9	7.2	3.3	0.1	1.9	29.5	0.7	2.2	0.5	0.8	0.6	1.7
SP	53.5	1.6	0.6	0.1	2.3	20.6	0.9	17.8	0.1	2.5	0.8	14.3
THI	5.5	1.2	1.5	0.1	10.5	69.3	0.9	5.0	0.1	5.8	12.6	73.8
VO	23.9	4.1	1.3	0.1	9.2	15.9	1.7	32.9	0.1	10.8	2.2	75.5
VSC	6.6	1.0	0.6	0.7	14.7	53.6	0.7	9.5	0.1	12.7	10.3	105.4
WC	28.8	5.1	7.4	0.7	5.2	35.5	1.8	5.7	6.5	3.4	1.4	10.2
WP	21.3	4.8	3.7	0.4	8.8	28.5	1.7	20.9	1.8	8.1	2.3	51.8

Table 4 - Characteristic points of TGA analysis.

Sample	$T_{ignition}$ (°C)	T_{peak} (°C)	$T_{reaction\text{-}end}$ (°C)
AS	171	296	791
BP	183	232	750
BRI	169	340	611
CC	233	478	775
CH	170	322	550
OS	195	289	609
OTP	180	325	548
PPLP	178	331	697
PL	183	318	506
PKS	194	333	716
RH	188	319	521
S	195	331	525
SP	170	287	619
THI	130	339	531
VO	182	269	804
VSC	195	324	550
WC	212	340	517
WP	200	332	631

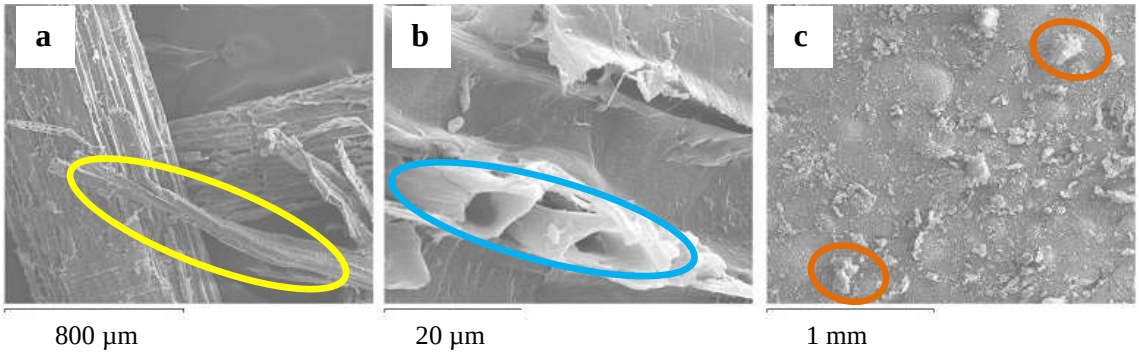

Figure 1. Wood chips SEM captures at room temperature (a x65 magnifications and b x2000) and after 550ºC burning (c x50 magnifications).

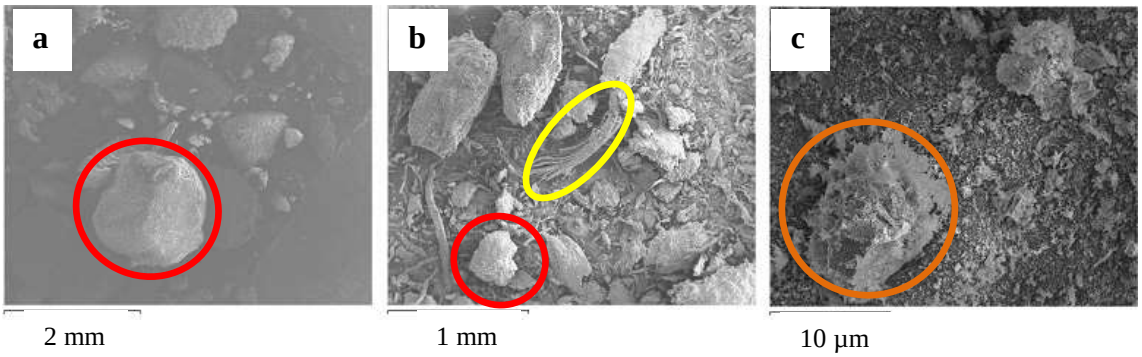

Figure 2. Pine kernel shell (a room temperature x20) and pine and pine-apple leaf pellets' (b room temperature x40 and c after 550ºC burning x350) SEM captures

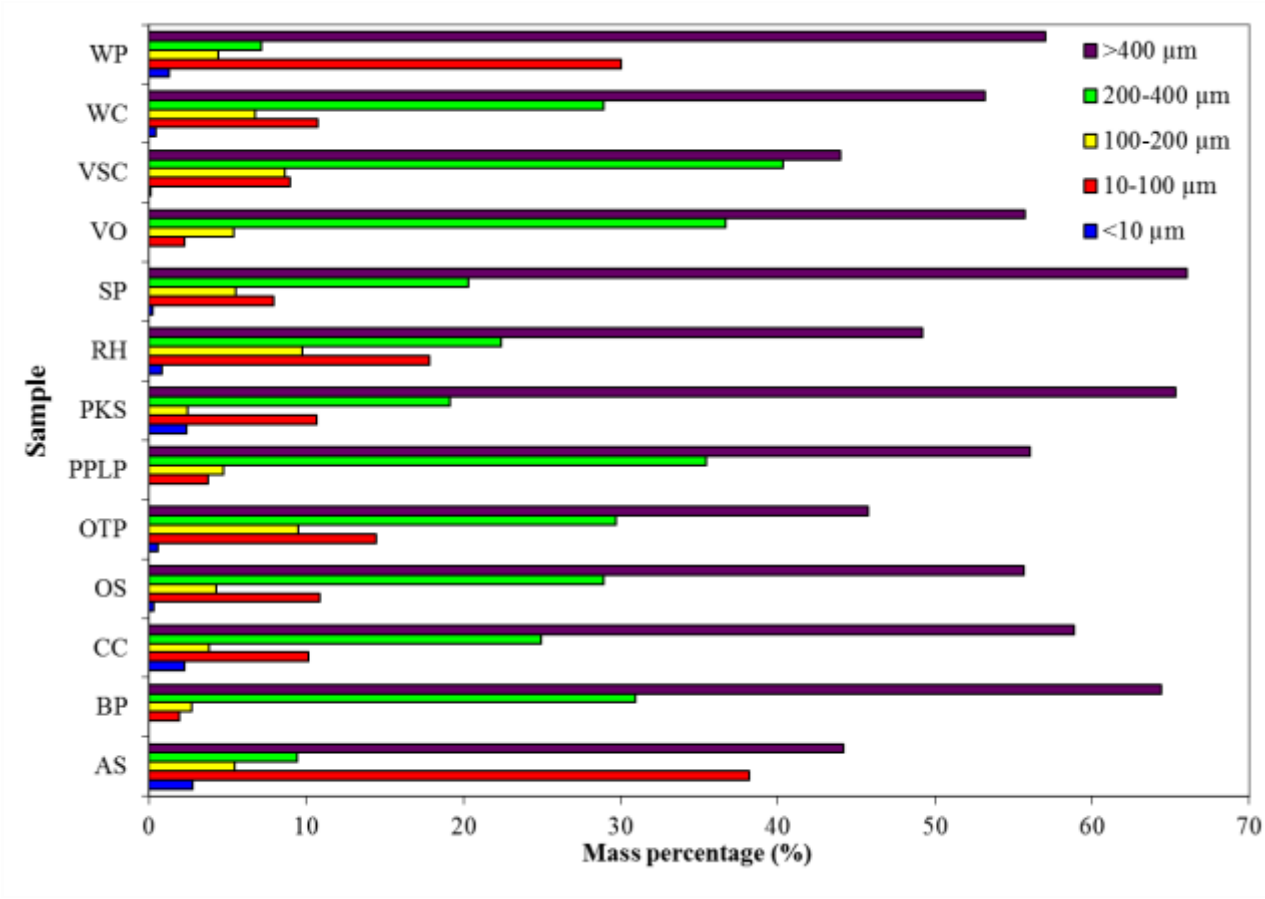

Figure 3. Particle size distribution of the selected biomass samples.

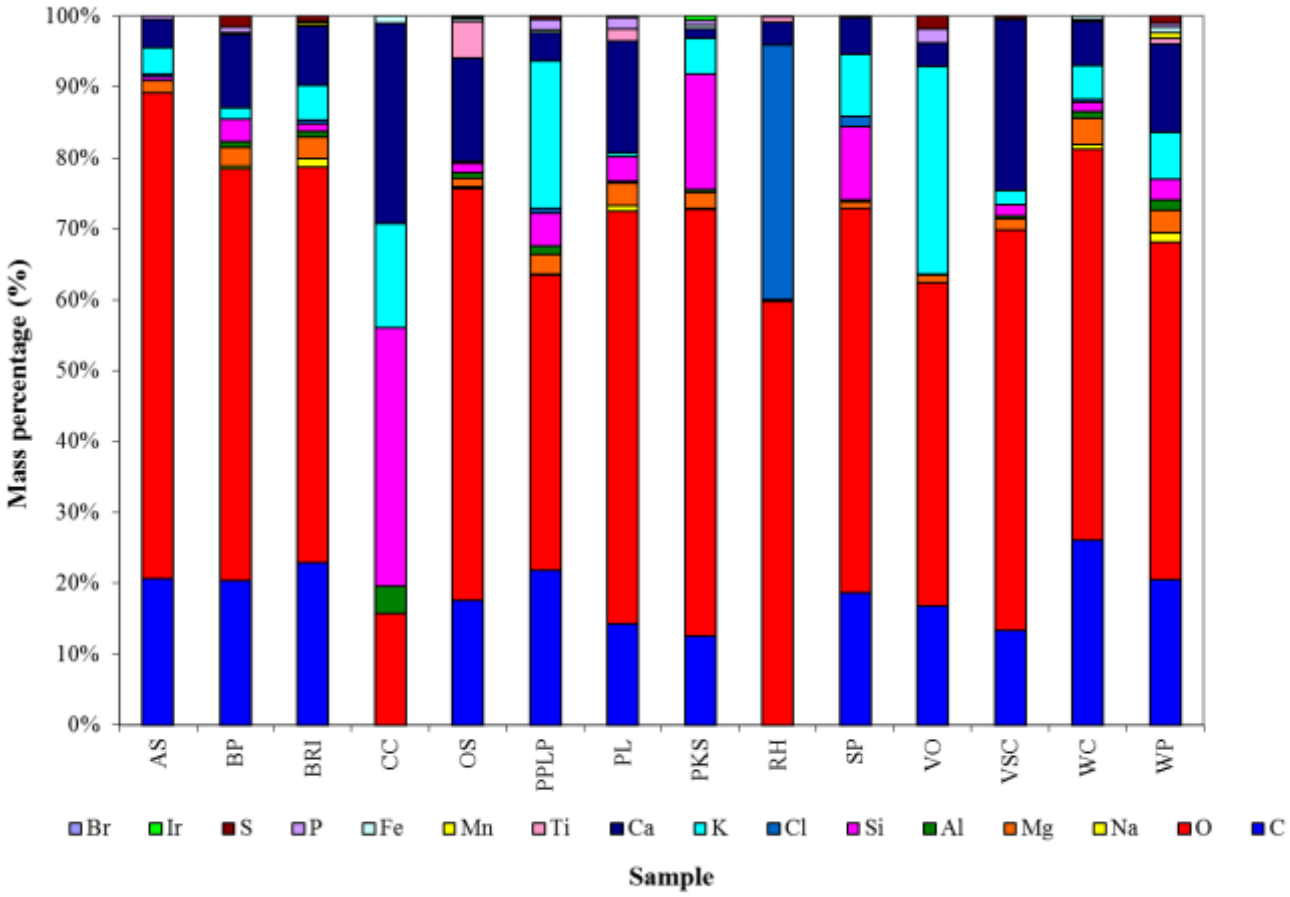

Figure 4. Results obtained from EDXA analysis.

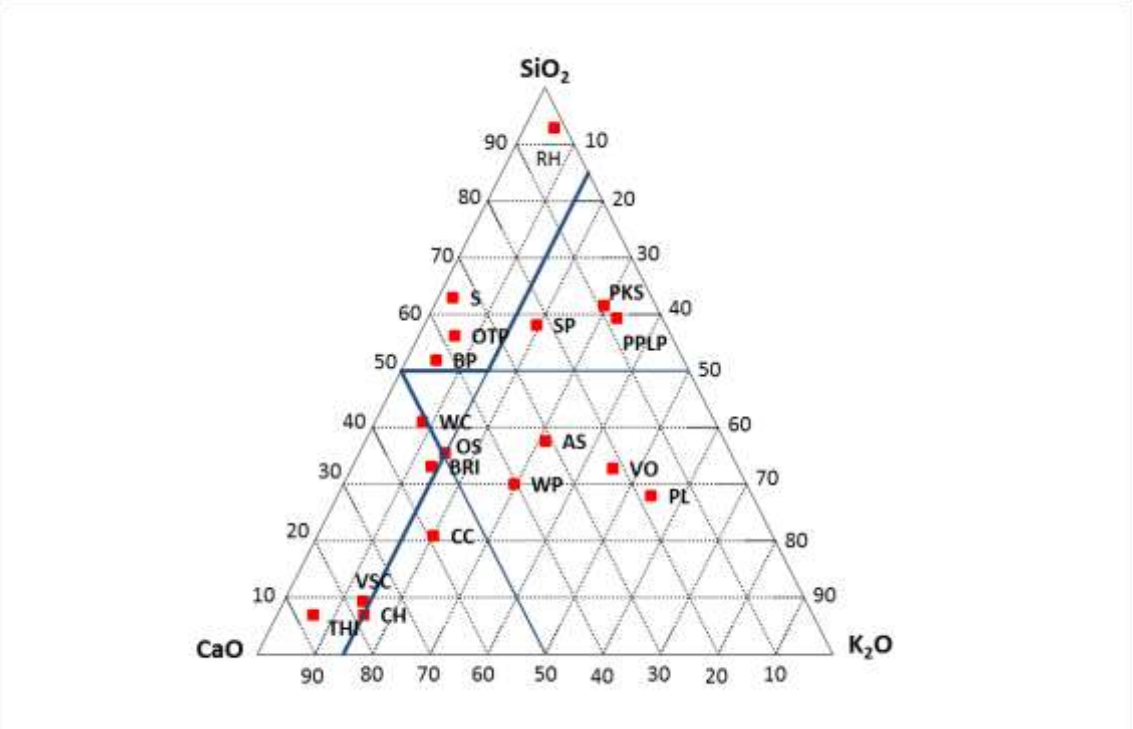

Figure 5. SiO_2-CaO-K_2O ternary diagram.

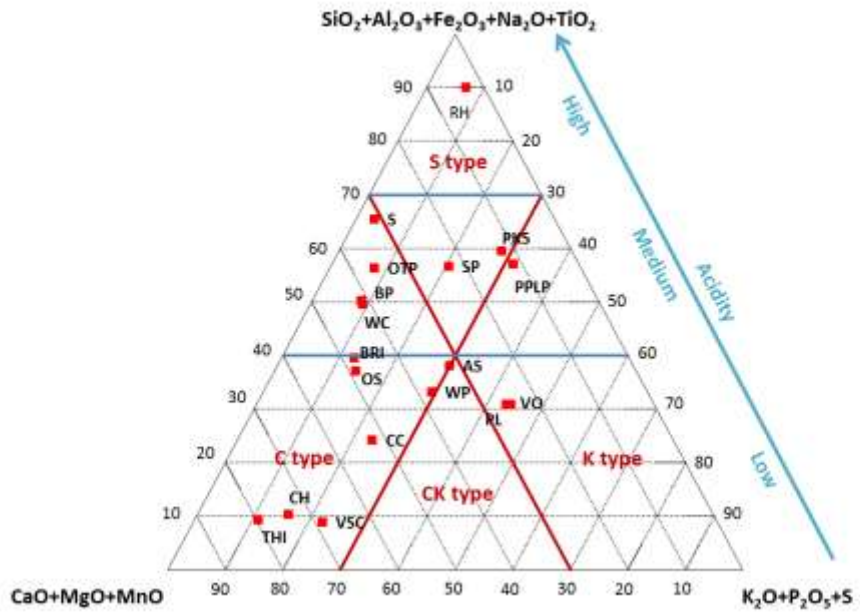

Figure 6. SiO_2+Al_2O_3+Fe_2O_3-+Na2O+TiO_2-CaO+MgO+MnO-K_2O+P_2O_5+S ternary diagram.

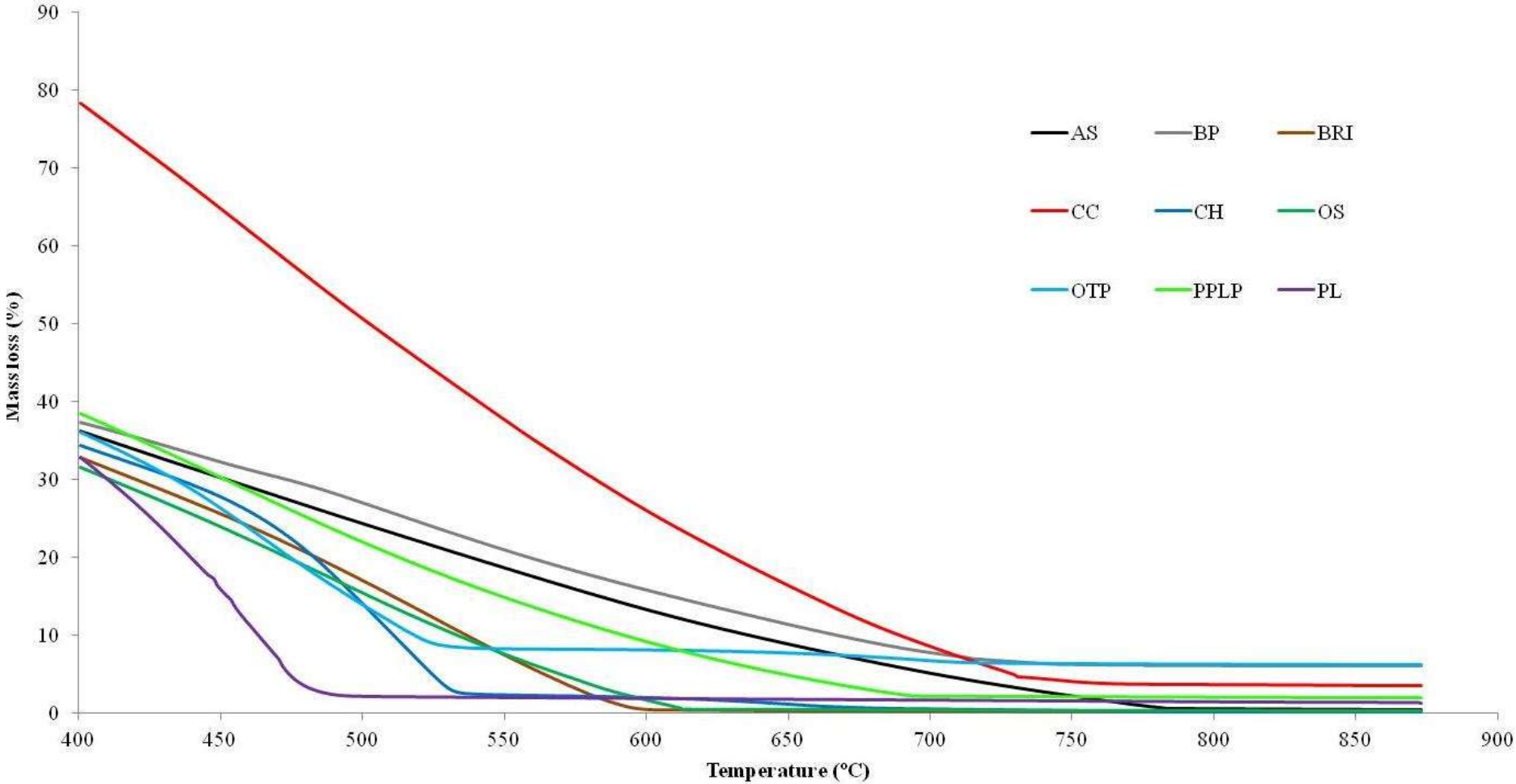

Figure 7. TGA profiles for several biomass samples from 400ºC (I).

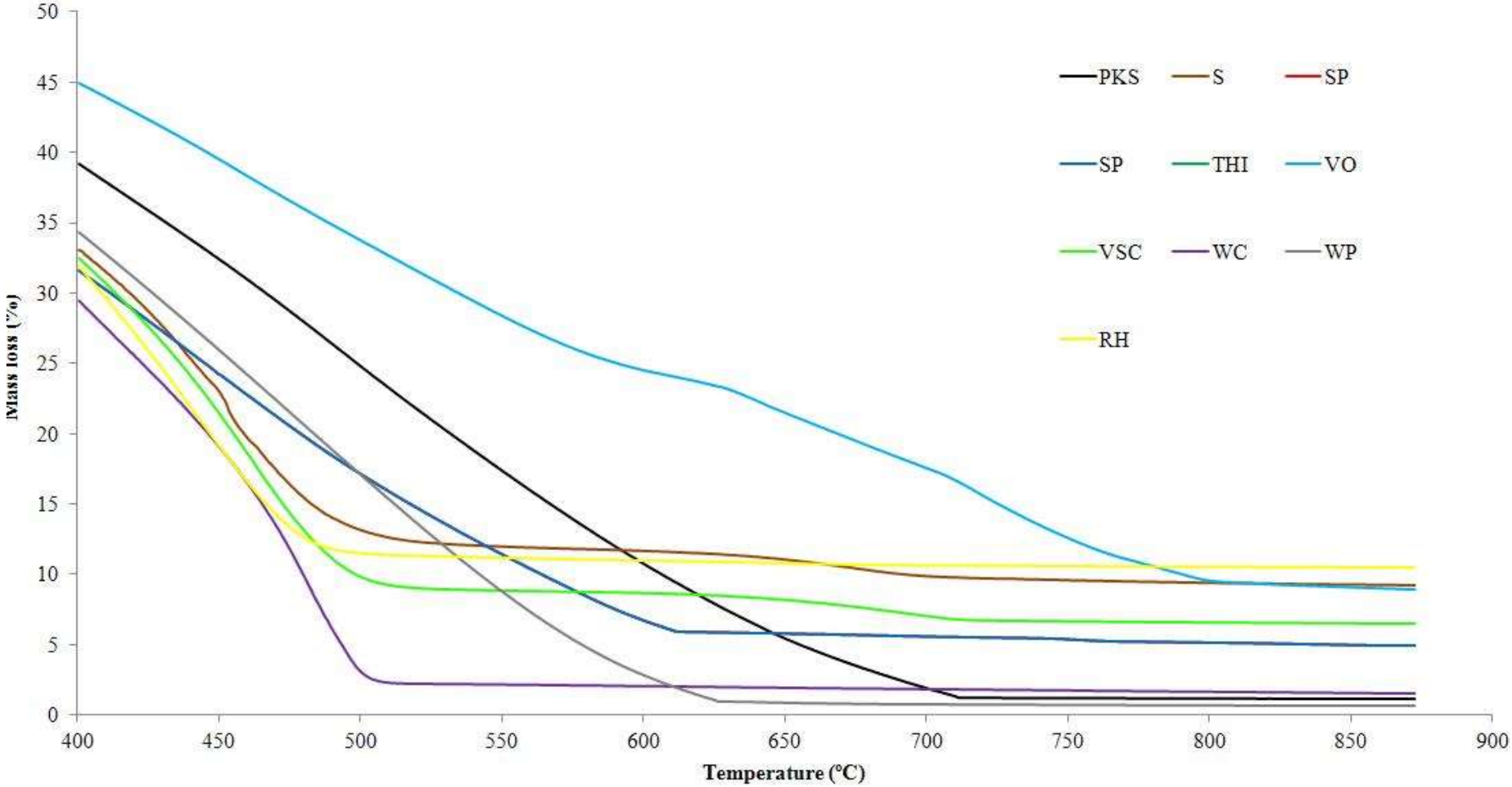

Figure 8. TGA profiles for several biomass samples from 400ºC (II).